Dalton Transactions

Accepted Manuscript

ROYAL SOCIETY OF CHEMISTRY

www.rsc.org/dalton

Cite this: DOI: 10.1039/c0xx00000x

www.rsc.org/xxxxxx

ARTICLE TYPE

Aqueous stability of alumina and silica perhydrate hydrogel: Experiments and computations

Yitzhak Wolanov,[a] Avital Shurki,[*,b] Petr V. Prikhodchenko,[*,c] Tatiana A. Tripol'skaya,[c] Vladimir V. Novotortsev,[c] Rami Pedahzur[d] and Ovadia Lev.[a]

Received (in XXX, XXX) Xth XXXXXXXXX 20XX, Accepted Xth XXXXXXXXX 20XX
DOI: 10.1039/b000000x

Alumina and silica perhydrate hydrogels were synthesized. Raman spectroscopy and solid ^{27}Al MAS NMR confirmed alumina perhydrate formation. Thermal and aqueous stability of alumina and silica perhydrates were studied showing exceptionally high stabilities. Alumina perhydrate retained some of the hydrogen peroxide even at 170°C, higher than any other reported perhydrate, whereas the silica perhydrate lost its hydrogen peroxide content already at 90°C. The silica perhydrate lost all its peroxide content upon immersion in water, whereas the alumina perhydrate was stable under near-neutral pH conditions. A computational study was conducted in order to glean molecular insight into the observed thermal and aqueous stability of alumina compared to silica perhydrate. Comparison of the hydrogen bond features and the stabilization energies of the hydrate and perhydrate of silica and alumina revealed a higher preference for hydrogen peroxide over water by alumina relative to silica. This is shown to be due to hydrogen peroxide being a better hydrogen donor than water and due to the superior hydrogen accepting propensity of alumina compared to silica.

Introduction

Hydrogen peroxide is a byproduct of the metabolic oxidation of aerobic organisms, and as such the H_2O_2 – H_2O ligand exchange, and the competing interactions of hydrogen peroxide on oxygen-containing surfaces are of fundamental importance. Preferential uptake of hydrogen peroxide over water influences biological mechanisms[1,2] and controls toxicity.[3]

Hydrogen peroxide is also an environmentally friendly, though mild oxidant. It is a less potent oxidant than the somewhat cheaper hypochlorous and nitric acids, but it forms minimal oxidation byproducts, and it does not require low pH conditions.[4] On the other side of the reactivity scale, hydrogen peroxide is much more reactive than dioxygen, and when activated it can either generate hydroxyl radicals and other potent active oxygen species, which are efficient organic cleansing agents, or dismutate to give water and dioxygen, which is important for water and soil bioremediation. Hydrogen peroxide is mostly marketed in aqueous solution. However, peroxide-rich solids are much in demand since they minimize transportation risks and catalytic dismutation of the hydrogen peroxide. There is also a need for controlled release of the hydrogen peroxide and in many cases the co-precipitate, be it a metal center or a ligand, can activate the peroxide and accelerate oxidative transformations.[5-7] Since water and hydrogen peroxide have a similar hydroxyl functionality and thus hydrogen bonding propensity, and there is large abundance of water compared to hydrogen peroxide under aqueous conditions, preserving the stability of hydrogen peroxide solids in aqueous solutions is a challenge.

Coarse classification of the available peroxide-rich solids shows four different categories which are characterized by two distinguishing criteria, hydrogels versus crystalline materials and peroxosolvates, i.e. materials containing undissociated H_2O_2, versus materials containing peroxo or hydroperoxo groups. Though this article involves only hydrogen peroxide containing gels, it is worthwhile to broaden the background to other forms of peroxides in order to illuminate the scarcity of peroxide sources with water stability.

Alkali metal peroxides (e.g. Na_2O_2) lose their peroxide content even under very basic conditions (highly basic conditions are irrelevant since they decompose H_2O_2), and the alkaline earth metal peroxides (e.g. CaO_2) retain their hydrogen peroxide only under very basic conditions (>pH 10). Most transition metal elements activate hydrogen peroxide and induce dismutation (Fe, Mn, Co, Ni, V, etc.)[8,9] and therefore, peroxocomplexes of transition elements are not stable. Some transition and p-block elements form stable peroxo- and hydroperoxocomplexes (e.g. B, Sb, Sn),[10,11,12] but water excess substitutes peroxo or hydroperoxoligands as was shown, for instance, for hydroperoxostannates[13]. These complexes also lose their peroxide content quickly under near neutral solutions.

We have shown recently that d^{10} transition metals are an exception and that crystalline zinc peroxide retains its peroxide content in aqueous solutions even under mild acidic conditions.[14,15] The exceptional stability of ZnO_2 was attributed to a combination of only one relevant oxidation state (+2) and the more covalent nature of the peroxide coordination to zinc. The

dissolution of hydroperoxo and peroxo compounds increases the pH (unless hydrolysis takes place), whereas hydrogen peroxide release by perhydrates has a much smaller pH effect, caused only by the release of the very weak H_2O_2 acid.

Inorganic perhydrates are well known and crystalline sodium percarbonate ($Na_2CO_3 \cdot 1.5H_2O_2$) is manufactured at several hundred tons per year mostly for bleaching[16] and also as a source of hydrogen peroxide in organic synthesis.[17] Urea peroxide $CO(NH_2)_2 \cdot H_2O_2$ is the most useful example of organic perhydrates.[18] It serves as an oxidizing agent, for disinfection, as an additive in numerous personal and health care products (acne treatment, teeth whitening, etc.) and for organic synthesis. [19-21] The propensity of amines to form crystalline perhydrates is rather common, and several amino acid perhydrates were synthesized and studied by our group.[22-24] However, all inorganic and organic peroxosolvates lose their hydrogen peroxide in water, and some of them even in organic solvents.[25]

Perhydrate hydrogels, the subject of the current research, are much less studied, though the versatility of the sol gel process allows control over the morphology, size and the composition of inorganic hydrogels,[26,27] and the high stability and low solubility of the metal oxides make them good carriers of hydrogen peroxide for environmental and catalytic applications.

Several reports regarding hydrogen peroxide induced polymerization of silica have been published.[28-30] Zeglinski et al.[29] loaded up to 68 wt% hydrogen peroxide into a silicate gel and demonstrated by FTIR studies and DFT calculations that hydrogen peroxide is held by hydrogen bonding. As far as we know, this is the only computational investigation of interactions between hydrogen peroxide and an inorganic gel. Peroxide induced polymerization of sodium metasilicates was also studied by ^{29}Si NMR spectroscopy, which allowed the authors to suggest that there is no peroxo- or hydroperoxo- coordination to the Si atom.[31] The silicate perhydrate also lost all its peroxide content in water.[30]

Several papers showed that the catalytic efficiency of epoxidation of hydrocarbons by hydrogen peroxide was improved by alumina[32,33] or aluminum salts.[6,34,35] It was suggested that the intermediate Al-OOH site is responsible for the activation of the hydrogen peroxide and oxygen transfer.[32,6] Others suggested that the activation of hydrogen peroxide is by the formation of hydrogen bonds between H_2O_2 and water in the second-coordination sphere of the aluminum ion.[34] Only one article claimed that alumina coordinates hydroperoxo (AlOOH) groups in the presence of peroxide, but the claim was not supported by experimental data.[36]

In this research we synthesized and studied a peralumina hydrogel by solid ^{27}Al MAS NMR and Raman spectroscopy, which confirmed perhydrate gel formation. Unlike persilica, the obtained peralumina hydrogel retained a significant amount of peroxide for a substantial period of time in aqueous solutions (> one month). Computational studies were then used to glean the underlying mechanistic difference responsible for the different behavior of the silica and alumina perhydrates.

Results

Preliminary studies: Aluminum perhydrate, AP and sodium aluminate perhydrate, SAP matrices retained most of their peroxide content after immersion in water. While sodium silicate perhydrate, SSP and silica perhydrate, SP lost their hydrogen peroxide content within less than an hour, although their initial peroxide concentration was very high, about 60 wt%. The results agree with previous studies of Zeglinsky[29,30] which showed that an exceedingly high concentration of hydrogen peroxide can remain entrapped within the SSP hydrogel when the gel is prepared from hydrogen peroxide rich solutions. The same qualitative trend was observed after ethanol washing. While the AP and SAP did not lose the hydrogen peroxide content, the SP and SSP lost most of their peroxide after 60 mL of ethanol wash.

A preliminary stability study was carried out to compare the air stability of AP and SAP hydrogels under the same conditions. The initial concentration of the hydrogen peroxide was 15-16 wt% in all tested aluminum hydrogels. The time traces of the hydrogen peroxide decomposition of SAP and AP at 30 and 5 ºC are shown in Figure S1 of the electronic Supplementary Information, SI. The AP showed a markedly better ability to retain hydrogen peroxide as compared to SAP. The higher decomposition rate of the aluminate perhydrate is attributed to the high local pH in the peraluminate hydrogel or to a higher level of impurities in the reagents. Therefore, further studies concentrated on AP, and the results are compared to the better studied persilica gels.

Morphology of the AP hydrogel nanoparticles: The AP hydrogel appears as a white powder. An alumina hydrate hydrogel that was prepared in an identical manner but with the addition of water instead of hydrogen peroxide solution has the same appearance. Alumina perhydrate nanoparticles were synthesized from aluminum-tri-sec-butoxide and hydrogen peroxide solution. An XHR-SEM image of the alumina perhydrate nanoparticles is shown in Figure 1(A). The image demonstrates spherically shaped nanoparticles of 40-150 nm diameter. A zoom at the surface of a single particle by HR-TEM is shown in Figure 1(B), which shows domains of different density.

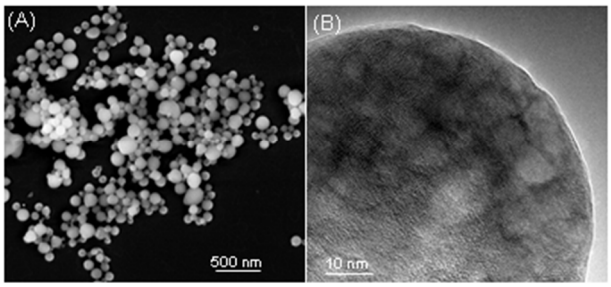

Figure 1: XHR-SEM image of alumina perhydrate, nanoparticles (A) and HR-TEM image of a single particle.

The nanoparticles were analyzed by permanganometry and found to contain about 9-10 wt% peroxide. Dynamic light scattering tests showed that the particles are nanodispersed with an average particle size of 200 nm, significantly larger than Figure 1(A) shows, probably due to some aggregation of the nanoparticles in the solution.

XRD studies reveal that AP is amorphous, whereas the alumina hydrate that was prepared in the same way was crystalline. The x-ray diffraction of alumina shows mainly the

diffraction pattern of Boehmite (more than 90%). The other crystalline component was Bayerite (no amorphous material was observed). The XRD diffractions of alumina hydrate and perhydrate are shown in the SI in Figure S2.

Structural characterization of the AP hydrogel was carried out by solid ^{27}Al MAS NMR and compared to the hydrate of alumina. The spectra of the two compounds are shown in Figure 2.

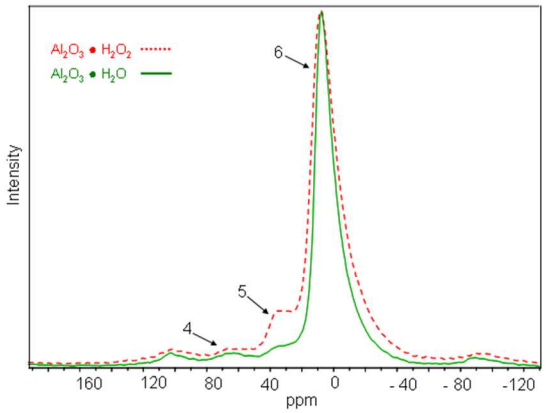

Figure 2: Solid 27Al MAS NMR of alumina perhydrate, AP (red) and hydrate (green). Coordination numbers are indicated.

The two spectra demonstrate a similar coordination environment of the aluminum atoms in the alumina perhydrate hydrogel and the alumina hydrate. The aluminum exhibits a resonance at 7 ppm and two smaller peaks at 35 and 67 ppm. The peaks at 105 and 90 ppm are spinning sidebands.[37] The resonance at 7 ppm agrees well with previous reports on the ^{27}Al NMR signal of six coordinated aluminum, and the small resonance peaks at 35 and 67 ppm are attributed to five and four coordinated Al, respectively.[37,38] Five coordination aluminum exists in solution at moderate pH [39] and some five coordinated aluminum was found also in alumina gel.[37] The higher intensity of the five coordination peak of AP compared to aluminum hydrate is interesting but its source remains obscure. The coexistence of four and six coordinated aluminum within the same powder was reported before and was attributed to stabilization of the four coordinated aluminum in Keggin type Al13 cation on the surface.[37] The existence of Keggin Al13 cation in alumina which was prepared from aluminum sec-butoxide was also reported. [40]

Raman spectroscopy is a sensitive method for studies of the coordination of peroxo groups, which is usually accompanied by a bathochromic shift relative to the 880 cm^{-1} line of free hydrogen peroxide.[41] The Raman spectra of AP and alumina hydrate are delineated in Figure 3. The AP spectrum (gray curve) exhibits a broad peak at 880 cm^{-1}, a region that is associated with (O–O) stretching vibrations.[42] This peak did not appear in the alumina hydrate spectrum (red curve) and disappeared after decomposition of the peroxide by heating the perhydrate to 300°C. The 880 cm^{-1} peak is broader compared to the sharp and symmetric line of hydrogen peroxide. For comparison, the spectra of aqueous hydrogen peroxide and silica perhydrate are shown in Figure S3 of the SI. The (O–O) stretching vibration of silica perhydrate has the typical sharp shape of the peroxide stretching vibrations at 876 cm^{-1}. The small shift to lower energies (compared to 880) is due to the hydrogen bonding of the hydrogen peroxide. The amorphous structure of the alumina allows very different modes of H_2O_2 bonding, which cause peak broadening of the O-O stretching vibrations of AP. We attribute the larger peak broadening of AP compared to SP to the stronger hydrogen bonds between the aluminum hydroxide and the hydrogen peroxide. The strength of the hydrogen bonding of silica and alumina will be addressed in details below.

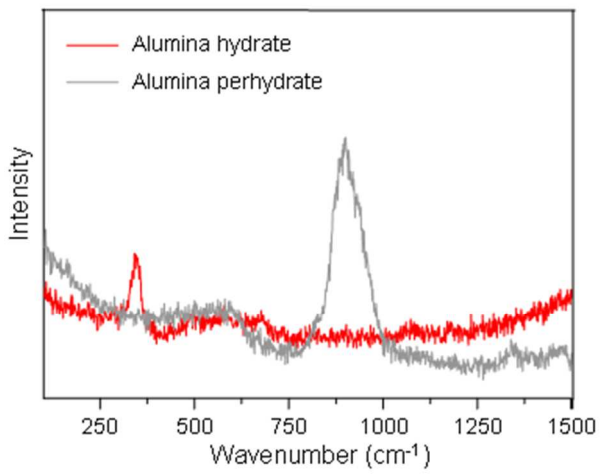

Figure 3: Raman spectra of alumina hydrate (red), and alumina perhydrate (gray)

A Raman line around 360 cm^{-1} is observed in the alumina hydrate only. This peak is characteristic to the Boehmite phase,[43] which agrees with the XRD diffractogram that showed that the crystalline phase of alumina hydrate is Boehmite.

Thermal stability: The thermal stability of AP (Figure 4A) and SP (Figure 4B) were studied by thermogravimetric analysis, TGA, differential scanning calorimetry, DSC and by titration with permanganate (permanganometry) as a function of temperature.

AP is stable up to 75°C based on the titrimetric studies. Then, a gradual loss of hydrogen peroxide starts, accompanied by a gradual weight loss, and an exothermic process begins at the same temperature. The exothermic process is attributed to the decomposition of hydrogen peroxide. Surprisingly, the hydrogen peroxide decomposition process continues up to 170°C. This can be seen by the peroxide loss, and by the weight loss. The heat release peaks already at 125°C, but this can be attributed to a balance between heat of evaporation of the bound water and the exothermic hydrogen peroxide decomposition.

The thermal analysis of SP (Figure 4B) shows that the perhydrate is stable up to 80°C, when a gradual weight loss starts. But the permanganate analysis reveals that silica perhydrate sharply loses 80% of its peroxide at 100°C. Since the peroxide loss curve is so steep for SP, the minimum of the DSC curve is delayed and the curve does not have a maximum. Likewise, the weight loss curve is steeper and terminates at 150°C. The temperature-dependent permanganometry analysis shows a much stronger stability of the alumina perhydrate compared to silica perhydrate. The SP and AP gel perhydrates cleavage is more

sluggish than the corresponding decomposition of the crystalline perhydrates. Serine perhydrate and sodium percarbonate lose their peroxide content by an autocatalytic process. The TGA of serine perhydrate and commercial sodium percarbonate are shown in Figure S4 of the SI. Serine perhydrate and sodium percarbonate lose all their peroxide content already at about 100°C, whereas the dismutation of AP continues gradually up to 170°C.

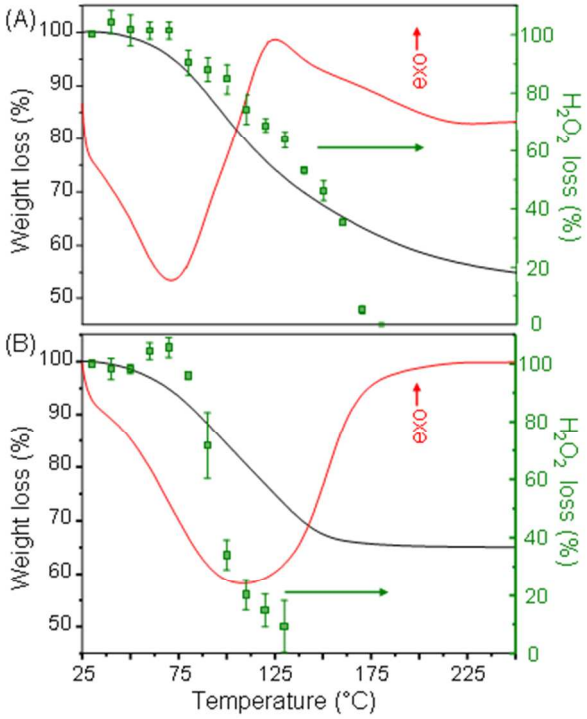

Figure 4: TGA (black), DSC (red) and peroxide content (green) as a function of temperature of alumina (A) and silica (B) perhydrates. Peroxide content data represent the average of three measurements, bars represent the standard deviation.

Perhydrates stability in water

Our preliminary studies showed that the there is a marked qualitative difference between AP and SP. SP lost all of its peroxide with either water or ethanol wash, whereas AP was much more stable.

In order to characterize the observed stability of alumina perhydrate in water more quantitatively, a kinetic study was conducted by immersion of the perhydrate in water and following the fraction of the retained peroxide in the filtered particles. Figure 5(A) presents the stability of alumina perhydrate hydrogel in tap water (pH 7.8) and in distilled water at different pH.

In distilled water, AP maintained more than 6 wt% of hydrogen peroxide in the first five hours, at the moderate pH range, and more than 4 wt% after 24 hours in the moderate acidic region. After this time, a sharp decrease in peroxide content was observed.

When AP was dispersed in tap water a stabilization effect was observed and the hydrogel retained more than 6 wt% peroxide after 72 hours and about 4-5% peroxide after more than 20 days (Figure 5A). We postulated that the loss of the hydrogen peroxide was due to the disintegration of the gel which partly dissolved and lost its hydrogen peroxide content. Apparently, tap water stabilized the gel structure. HR-SEM revealed that the morphology of the gel was indeed altered after 24 hours of immersion in distilled water and an open sheet-like structure appeared, whereas in tap water the dense structure of the AP hydrogel was maintained. The HR-SEM images of the hydrogel before and after 24 hours in distilled water and in tap water are shown in Figure S5 in the SI.

In order to study the hydrogen peroxide retention of a stabilized AP which behaves like alumina in tap water we added phosphate ions to the test solution. The adsorption of phosphate on alumina surfaces is amply reported.[44-46] Phosphate ions were found to have high affinity for alumina compared to other ions,[46] their adsorption is pH dependent,[44] and several studies found that this attachment involved coordination with the aluminum atoms.[45,47] We used a constant 4 mM phosphate to all test beakers and adjusted the pH by addition of HCl and NaOH solutions. The stabilization of alumina perhydrate by phosphate over a wide pH range is shown in Figure 5(B).

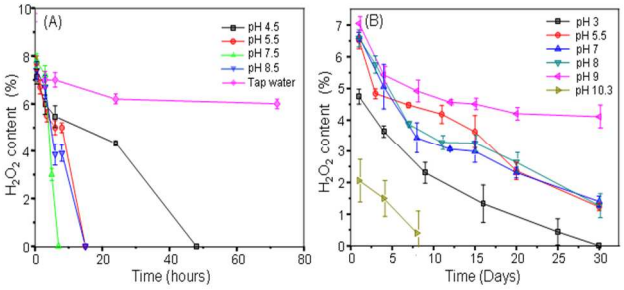

Figure 5: Peroxide content of AP hydrogel as a function of time at different pH. (A) AP immersed in distilled water corrected to the specified pH by addition of HCl and NaOH and in tap water, pH 7.8 (B) AP immersed in 4mM phosphate buffer solution, corrected to the specified pH by addition of HCl or NaOH

In the presence of phosphate buffer, a superior stability was observed over a wide pH range. At the extreme points of the studied pH range, i.e. at pH 3 & 10.3, the peroxide loss rate was highest. The highest stability was obtained at pH 9. At this pH, AP retained about constant 5 wt% peroxide after 30 days.

The gradual decrease in the peroxide content of AP in the range of pH 5.5 - 8 is probably a result of bridging of the alumium hydroxide surfaces within the gel by the negatively charged (coordinated) phosphate ions. At the higher pH, the alumina surface became increasingly negatively charged, and the adsorption/coordination of the phosphate decreased, [46] and thus the stability of the particles decreased. Once the gel is stabilized, the affinity of the hydrogen peroxide to the aluminum hydroxide becomes the most important stabilization, and this is improved as the pH rises and the surface is deprotonated, thereby increasing the stability of hydrogen bonding to H_2O_2 hydrogen donors. At the high pH (10.3), hydrogen peroxide instability becomes dominant.

The alumina perhydrate nanoparticles followed a similar behavior as of the AP hydrogels. The nanoparticles lost all their peroxide content after 24 hours in distilled water and maintained

about 3 wt% of peroxide after more than 20 days in the phosphate solution. The structural decomposition of the nanoparticles as a function of time in distilled water is shown in Figures 6(A), 6(B) and 6(C). And the stability of the nanoparticles structure as a result of phosphate adsorption is shown in Figures 6(D),6(E) and 6(F).

The lower stability of the nanoparticles compared to the gels, is not only the result of a kinetic effect. We believe that the higher surface energy of nanoparticles constitutes an additional driving force for dissolution.[48]

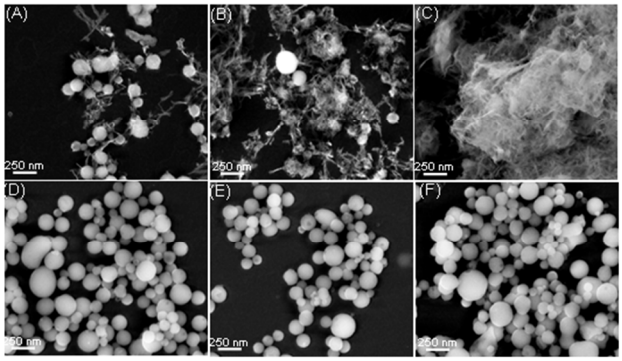

Figure 6: XHR-SEM images of alumina perhydrate nanoparticles after dispersion (0.03%) in distilled water for 1 day (A), 3 days (B), 7 days (C). And after immersion in 4 mM buffer phosphate at pH 9 for 1 day (D), 3 days (E) and 7 days (F).

Biocidal activity

The biocidal activity of the AP hydrogel was qualitatively demonstrated by the zone inhibition test. Tablets of alumina perhydrate (A), alumina perhydrate after heating at 300°C (B) and alumina hydrate (C) were incubated in sterile Petri dished contained cultivation of *red Streptoverticillium reticulum* on agar, and typical results are shown in Figure 7:

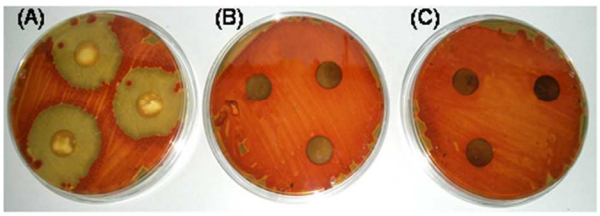

Figure 7: Cultivation of *red Streptoverticillium reticulum* on agar incubated with tablets of alumina perhydrate (A), alumina perhydrate after heating at 300°C (B) and alumina hydrate (C)

It is clearly seen that while samples B and C which did not contain hydrogen peroxide show no biocidal activity, sample A of alumina perhydrate served as stable source of hydrogen peroxide and zones of inhibition are observed.

Computational Study

As mentioned in the introduction, in a previous theoretical study, Zeglinski[29] successfully proved the formation of strong hydrogen bonds between silica dimer and hydrogen peroxide. Zeglinski, however, did not compare the affinity of water and hydrogen peroxide to the silica surface.

In the present work, we wanted not only to prove the possible formation of hydrogen bonds by energy considerations, but also to compare the affinity of H_2O_2 and H_2O to silica and alumina models. For this purpose, structures were optimized in a simulated aqueous solvent at the MP2 level of calculation as described in the experimental part, and the affinity was estimated by the interaction energy. In addition, we calculated the stabilization energies of the complexes in order to consider also the changes due to the deformation of the fragments during complex formation.

Figure 8 presents typical structures of alumina perhydrate (1 and 2) along with alumina hydrate (3). Both H_2O_2 and H_2O act as hydrogen bond (HB) donors in their interaction with the hydroxyl groups, which are coordinated to the aluminum and as HB acceptors in their interaction with the water groups within the alumina. The H_2O_2 can form two-three HBs with the alumina dimer, whereas H_2O can form up to two HBs.

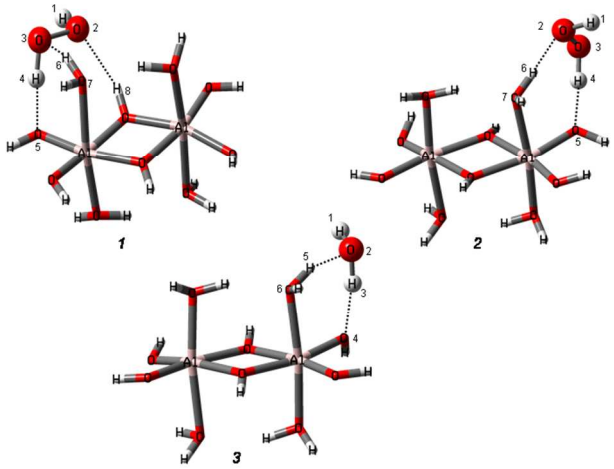

Figure 8: Typical low energy structures of alumina dimer complexed with H_2O_2 (1 and 2) and H_2O (3). For convenience, the alumina dimer is presented by sticks while H_2O_2 and H_2O are presented by balls and sticks

Interaction, ΔE_{IE}, and stabilization, ΔE_{SE}, energies due to hydrate/perhydrate formation are summarized in Table 1 (entries 1-3). Interaction energies reflect mainly the energy reduction due to HB formation. Stabilization energies, on the other hand, in addition to HB formation, consider also changes in energy due to the deformation of the fragments during complex formation, as mentioned above.

Alumina is aquated, yet the identity of the exact dielectric constant that properly defines it is not clear. Therefore, stabilization and interaction energies were calculated both in vacuum and in aqueous solution, thus covering a large range of possible dielectric constants. The results clearly show that the alumina perhydrates (structures 1 and 2) have higher stabilization and interaction energies than the corresponding hydrate (structure 3). We note in this respect that this is typical for most of the structures obtained and not only for the lowest energy structures

(data not shown). Overall, the results are seen to be consistent and usually do not depend on the dielectric constant used to define the system. Therefore, one can clearly state that the calculations suggest that alumina is stabilized more when interacting with hydrogen peroxide as compared with water. In other words, energetically, alumina prefers to interact with hydrogen peroxide over water. This explains, therefore, the relatively high stability of alumina perhydrate in water.

As mentioned earlier, one of the typical structures of alumina perhydrate (structure 1) exhibits three HBs compared with only two in alumina hydrate. This may provide a partial explanation for the origin of the higher stabilization. However, structure 2 exhibits only two HBs and yet its stabilization energy is higher as compared with structure 3.

Table 1: Stabilization and interaction energies of the alumina and silica dimers complexed with hydrogen peroxide or water molecules

Structure[a]	aqueous solution		Vacuum	
	ΔE_{SE}	ΔE_{IE}	ΔE_{SE}	ΔE_{IE}
1	-13.3	-16.5	-19.2	-25.2
2	-13.3	-15.5	-17.0	-21.2
3	-10.4	-12.9	-15.8	-19.5
4	-8.3	-9.9	-12.1	-12.8
5	-7.8	-8.5	-12.4	-11.2
6	-7.8	-8.6	-12.9	-11.9

[a] Structure numbering is based on Figures 8 and 9.

In order to understand these trends in the stabilization energies, various key distances and angles in each structure are listed in Table 2. Examination of the HB angles reveals that structure 2 exhibits HB angles which are closer to the optimal 180º suggesting it may contribute to stronger HB.

Inspection of the HB lengths is even more instructive. When H_2O_2 serves as HB-donor within perhydrates (first two entries) the resulting HB lengths are about r_{donor} =1.51±0.01Å. Such distances are usually indicative of strong HBs.[49] When H_2O_2 serves as HB-acceptor, on the other hand, the resulting HB lengths are longer by >0.20Å (5th column in Table 2). Therefore, the results suggest that H_2O_2 as a donor forms HBs which may be stronger than the HBs that it forms as an acceptor. Bond length, however, does not always correlate linearly with bond strength. Thus, to support this suggestion we calculated the electron density at the HB critical point, $\rho(r_c)$ using Bader's theory of atoms in molecules (AIM). These densities are known to increase linearly with increasing stabilization or HB energy.[50-52] That is, higher electron densities were shown to associate with stronger HBs. The $\rho(r_c)$ values of the HBs with H_2O_2 as a donor (≥0.063 au) are significantly larger than those with H_2O_2 as an acceptor (≤0.039 au), suggesting that they are indeed stronger. These results imply that in this case the trends in HB length also correlate with the HB strength as was recently suggested.

Within alumina hydrates, on the other hand, (structure 3) the situation is different. Here as can be seen from Table 2 (entry 3), the bond lengths of both H_2O as a donor and as an acceptor are very similar (1.62±0.04Å). Likewise the computed values of electron density, $\rho(r_c)$, at the HB critical point of the two bond types, are quite similar. These results suggest in turn that the bond strength is also similar.

This phenomenon of H_2O_2 presenting stronger HBs as donor in perhydrates compared to both H_2O_2 as HB acceptor in perhydrates and to H_2O as both donor and acceptor in hydrates was already pointed out in a recent study of amino acid perhydrates.[24] The authors showed that when hydrogen peroxide acts as an H donor (in HBs) it forms shorter O…H-O distances (by more than 0.1 Å) than water donors in the amino acid hydrates. However, when hydrogen peroxide acts as an acceptor there is no significant difference between its O…H-O distance and that of water. The difference in the bond strengths was attributed to the acidic character of H_2O_2. H_2O_2 with a pK_a of 11.75 is much more acidic than H_2O with pK_a = 14. As a result, HBs of H_2O_2 as donors are shorter and stronger than HBs of H_2O as donor.

In summary, the donor HBs of H_2O_2 which are stronger than those of H_2O (due to the higher acidity of hydrogen peroxide) along with the number of HBs which can be higher with H_2O_2 and the more optimal HB angles (due to additional degree of freedom of the rotation around the O-O bond), contribute to higher stabilization in the formation of alumina perhydrate as compared to alumina hydrate, leading to the relatively high stability of alumina perhydrate in solution.

Table 2: Key structural HB parameters for alumina and silica perhydrates and hydrates.

Structure	H_2O_2/H_2O HB Donor			H_2O_2/H_2O HB Acceptor		
	r_{donor}(Å)	∠ (deg)	$\rho(r_c)$[a] au	$r_{acceptor}$(Å)	∠ (deg)	$\rho(r_c)$[a] au
1	$H_4\cdots O_5$: 1.52	$O_3-H_4\cdots O_5$: 168	0.069	$O_3\cdots H_6$: 1.79	$O_3\cdots H_6-O_7$: 154	0.034
				$O_2\cdots H_8$: 1.96	$O_2\cdots H_8-O_9$: 153	0.022
2	$H_4\cdots O_5$: 1.51	$O_3-H_4\cdots O_5$: 177	0.063	$O_2\cdots H_6$: 1.72	$O_2\cdots H_6-O_7$: 172	0.039
3	$H_3\cdots O_4$: 1.62	$O_2-H_3\cdots O_4$: 160	0.052	$O_2\cdots H_5$: 1.66	$O_2\cdots H_5-O_6$: 161	0.046
4	$H_4\cdots O_5$: 1.84	$O_3-H_4\cdots O_5$: 165	0.029	$O_2\cdots H_6$: 1.90	$O_2\cdots H_6-O_7$: 156	0.026
	$H_1\cdots O_8$: 1.84	$O_2-H_1\cdots O_8$: 166	0.029			
5	$H_4\cdots O_5$: 1.74	$O_3-H_4\cdots O_5$: 171	0.035	$O_3\cdots H_6$: 1.78	$O_3\cdots H_6-O_7$: 171	0.033
6	$H_3\cdots O_4$: 1.84	$O_2-H_3\cdots O_4$: 168	0.027	$O_2\cdots H_5$: 1.73	$O_2\cdots H_5-O_6$: 174	0.038

[a] ρ(rc) values are based on the MP2 wavefunctions..

Discussion

Peralumina is one of the rare cases of a perhydrate hydrogel, and its high aqueous stability makes it unique. Whereas we and others have shown several hydroperoxo and peroxo non-crystalline materials,[11,13] inorganic peroxosolvates are rare, and as far as we can tell, the only inorganic perhydrate gels are silica and alumina based hydrogels. We base our conclusion that peralumina is a molecular adduct of alumina and hydrogen-peroxide mainly on the Raman ν(O-O) vibration peak. Coordination to alumina should have resulted in >10 cm^{-1} bathochromic Raman shift similar to peroxostanate,[13,53] peroxoborate[54] and peroxoantimonate.[11]

The analogy between column 13 elements supports our conclusion regarding the formation of peroxosolvate of alumina. Mayer [55] has demonstrated that perchlorate ligand in gallium porphyrinate is not substituted by excess hydrogen peroxide, thus concluding that hydrogen peroxide is a very weak metal ligand in acidic media. The same conclusion was also reached for non-aqueous hydrogen peroxide solutions of gallium and indium hexafluoro complexes by Kirakosyan et al.[56] Boron, another column 13 element, forms peroxocomplexes only at pH>7 and does not interact with hydrogen peroxide under acidic conditions.[57] Thallium catalyzes the decomposition of hydrogen peroxide and thus is irrelevant. Therefore, it can be generally concluded that all column 13 elements do not coordinate hydrogen peroxide in the absence of a base, as rightly stipulated based on gallium studies alone by Mayer.[55]

Additionally, a mixture of aluminum t-butoxide did not form a gel (in more than 30 minutes) in the presence of pure (>99.4 wt%) hydrogen peroxide, at least not until not sufficient water was formed by hydrogen peroxide decomposition. So in line with Mayer's conclusion, the sol-gel reaction of aluminum t-butoxide with aqueous hydrogen peroxide proceeds through hydrolysis (alumina gel formation) and subsequent adduct formation with hydrogen peroxide.

We can now explain based on the computational studies why silica perhydrate is not as stable as alumina perhydrate in water. Figure 9 presents typical structures of silica perhydrate (4 and 5) along with silica hydrate (6). H_2O_2 and H_2O form HBs with the hydroxyl groups, both as donor and as acceptors. Like in alumina, H_2O_2 can form two-three HB with the silica dimer, whereas H_2O can form up to two HBs.

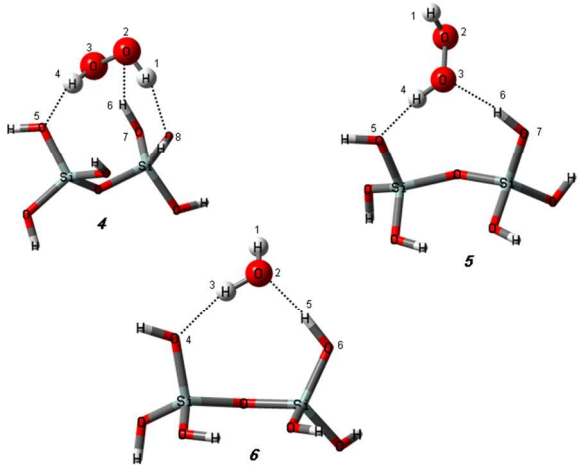

Figure 9: Typical low energy structures of silica dimer complexed with H_2O_2 (4 and 5) and H_2O (6). For clarity, the silica dimer is presented by sticks while H_2O_2 and H_2O are presented by balls and sticks.

The stabilization and the interaction energies of both silica hydrate and perhydrate are significantly lower than those of alumina (Table 1 entries 4-6 compared with entries 1-3). Thus, overall the interactions with silica are weaker, leading to complexes which are less stable. Moreover, different from alumina, the stabilization energy due to silica perhydrate formation is very similar to the stabilization energy due to silica hydrate formation, suggesting that in aqueous solution, which involves large excess of water molecules (compared with H_2O_2), silica perhydrate will not be favored.

The geometrical parameters of SP, which are in good agreement with Zeglinski's work,[29] provide a partial explanation for these trends. Similar to alumina, both H_2O_2 (structures 4 and 5) and H_2O (structure 6) form donor and acceptor HBs with the hydroxyl groups of the silica dimer. However, overall the HBs with silica (≥1.7 Å) are much longer than those of alumina. These longer HB lengths are also accompanied by smaller electron densities at the HB critical point ($\rho(r_c)$) suggesting that silica forms much weaker HBs. We note in this respect that multiple HBs (e.g., structure 4 where silica involves 3 rather than 2 HBs with H_2O_2) usually result in even longer and weaker bonds, leading therefore to no significant energy gain.

Furthermore, the difference between the HB length of H_2O_2 as donor and acceptor is diminished, and is comparable to that of H_2O. In fact, for H_2O this difference even inverted, exhibiting somewhat shorter HBs for H_2O as acceptor compared to donor. These trends, again, nicely correlate with $\rho(r_c)$ values, suggesting that the advantage of H_2O_2 having a strong HB as a donor, is missing and the interactions of H_2O_2 with silica are thus, comparable with those of water.

The computational studies underscore the similarity between the crystalline perhydrates that were amply studied by our group: [22-24] HBs in which the H_2O_2 acts as a hydrogen donor are stronger than HBs of H_2O acting as H-donor, whereas H_2O_2 H-accepting propensity is not significantly different from water. Hydrogen bonds with H_2O_2 hydrogen donor are in general shorter (based on crystalline structures)[24] and stronger (based on molecular computations) [22] than the corresponding bonds of water and the hydrogen bonding with hydrogen peroxide acting

as hydrogen acceptor.

Despite this similarity between crystalline and hydrogel perhydrates there are also some differences. The Raman □□O-O) vibration frequency reflects the strength of the hydrogen bonding. Broadening of the Raman peak of the O-O stretching was observed for AP but not for SP (Figure 3 and S3 in the SI). The broadening is attributed to HB formation and shows that the HB of hydrogen peroxide with AP spans a large distribution of HB strengths, at least some of which are considerably stronger than in SP. This is also revealed in the computational studies which show that some of the HBs between hydrogen peroxide and alumina involve shorter bond lengths than the bonds of H_2O_2 with silica whereas others, particularly those in which hydrogen peroxide acts as an H acceptor are of similar length and energy for persilica and peralumina (Table 2, columns 2 and 5).

AP was found to be more stable than SP, both in terms of thermal as well as aqueous stability. The thermal stability of AP is much superior to SP, and some peroxide is retained in AP even at 175°C. The thermal response reflects the energetics of a process involving bound peroxide decomposition and evaporation of the water product.

$$\equiv AlOH\circ H_2O_2 \rightarrow \equiv AlOH + 0.5O_{2\,(g)} + H_2O_{\,(g)} \qquad (1)$$

The TGA response of the gels (AP as well as SP) is much more sluggish than the dismutation of crystalline perhydrates (see for example the DSC response of serine perhydrate and commercial sodium percarbonate (Sigma) carried out under identical conditions, Figure S4 in the SI). This can be partly attributed to the lower loading of the peroxide in the gels compared to crystalline material but also to the more heterogeneous surrounding of the bound hydrogen peroxide in the gel, which results in a wide range of HB bonding energies, different number of bondings and evaporation energy (of bound water and the H_2O product) from the heterogeneous matrix. The first two are reflected in our computation studies whereas the latter requires unattainable many-atoms computation.

The aqueous stability is a different type of stability, because it reflects water – hydrogen peroxide exchange,

$$\equiv AlOH\circ H_2O_2 + H_2O \rightarrow \equiv AlOH\circ H_2O + H_2O_2 \qquad (2)$$

and it is also affected by the stability of the peralumina network, as shown by the increased stability of peralumina in the presence of phosphate stabilizer.

Indeed, aqueous stability does not necessarily correlate with thermal stability. All reported peroxosolvates (e.g. sodium percarbonate) release H_2O_2 promptly under near neutral pH conditions regardless of their thermal stability. The lack of correlation between the two types of stability is also apparent for the isostructural ZnO_2 and MgO_2: the former has higher aqueous stability[14], whereas the latter is thermally more stable.[58]

Experimental Section

Synthesis protocols

Sodium aluminate perhydrate hydrogel (SAP): 1M solution of sodium aluminate was prepared by dissolving 0.82g of sodium aluminate (Fisher, UK) in 10 mL of distilled water. 4 mL of 55 wt% hydrogen peroxide (Makhteshim, Israel) were added to the prepared solution to obtain immediate gelation. Hydrogel preparation: The gel was dried for 24h in vacuum or by washing two times in ethanol and once in diethyl ether and then dried for 2 hours in vacuum.

Alumina perhydrate (AP): 4 mL of 55 wt% hydrogen peroxide were added to 2.4g Aluminum-tri-sec-butoxide 99% (Aldrich) during mixing to obtain immediate gelation. Hydrogel preparation: The gel was dried for 24h in vacuum or by washing two times in ethanol and once in diethyl ether and then dried for 2 hours in vacuum.

Sodium silicate perhydrate (SSP): A 1M solution of sodium silicate was prepared by dissolving 2.84g of sodium metasilicate nonahydrate (Sigma, Israel) in 10 mL of distilled water. 4 mL of 55 wt% hydrogen peroxide were added to the prepared solution. Gelation occurred after 1 hour. Hydrogel preparation: The gel was dried for 24h in vacuum or by washing two times in ethanol and once in diethyl ether and then dried for 2 hours in vacuum.

Silica perhydrate (SP): 1.5 mL of tetraethoxysilane **(**Aldrich**)** were dissolved in 2.85 mL ethanol (Biolab, Israel). 2.55 mL of 55 wt% hydrogen peroxide were added to the prepared mixture to obtain a clear solution. Then, 25 µL of concentrated NH_4OH solution (Biolab, Israel) were added during mixing to obtain the perhydrate gel after a few minutes. Hydrogel preparation: The gel was dried for 24h in vacuum or by washing two times in ethanol and once in diethyl ether and then dried for 2 hours in vacuum.

Hydrate gels and hydrogels of silica, sodium silicate, alumina and sodium aluminate were prepared in an identical manner but with the addition of water instead of hydrogen peroxide solution.

Alumina perhydrate nanoparticles (APNp) synthesis: The synthesis protocol is based on a previous report[59] for the preparation of α-Al_2O_3 nanoparticle with some modifications. 300 mg of aluminum-tri-sec-butoxide were dissolved in 40 mL of anhydrous octanol (Acros) at 70 ^oC. NH_3 gas was bubbled through 2 mL of 55 wt% hydrogen peroxide in order to increase the pH of the hydrogen peroxide solution without dilution. The process was done in an ice bath to prevent heating and dismutation of the hydrogen peroxide. Then, 2 mL of the H_2O_2/NH_4OH mixture were dissolved in 200 mL acetonitrile (Biolab, Israel). The acetonitrile solution was then mixed with the octanol solution during stirring and a stable dispersion of the alumina perhydrate nanoparticles was immediately obtained. After 15 s of stirring, the dispersion was left to stand unstirred for another 15 s, and then the nanoparticles were separated by centrifugation at 5,000 rpm for 15 min, washed twice with ethanol and then once again with diethyl ether and finally dried under vacuum for 1 hr.

Preparation of 99.4 wt% hydrogen peroxide. The hydrogen peroxide was prepared from serine perhydrate crystals according to our previously reported protocol.[25]

Determination of the peroxide content. The amount of active oxygen in the solids and solution were determined by filtration of the solids and immersion in distilled water and then titration was carried out with freshly prepared 0.01N potassium permanganate solution.[60] The accuracy of the method is within 1-2%.

Stability studies: 90 mg of alumina perhydrate hydrogel were dispersed in 300 mL distilled water and in 4 mM buffer phosphate solutions at different pH. pH control was achieved by changing the ratio between the sodium phosphate monobasic (Mallinckrodt Baker, US) and di-sodium hydrogen phosphate (Merck, Germany), or by addition of 1M solutions of HCl or NaOH.

Constant volumes were sampled out under mixing, and then the alumina hydrogel was separated by centrifugation. The alumina hydrogel was washed one time with ethanol and one time with diethyl ether and left to dry at room temperature. The amount of peroxide in the hydrogel was measured by permanganometry.

Biocidal activity study: 150 mg of the tested powder was manually compressed using a KBr hydraulic press at a pressure of 1 ton, to obtain tablets with 13 mm diameter and 1 mm thickness.

The biocidal test was performed according to ASTM E1428 – 99. In summary, an agar inoculated with *Streptoverticillium reticulum* was introduced into sterile Petri plates. The test tablets were placed, three to a plate, on the agar surface and incubated at 30 ^{o}C for 14 days.

Analytical Instruments

^{27}Al MAS NMR study was performed on a Bruker Avance 400 NMR pulse spectrometer using a commercial 4-mm MAS probe head. The spectra were acquired at a Larmor frequency of 104.3MHz. The spinning rate was 10 kHz. A $\pi/12$ single pulse was used to obtain the MAS spectra. The recycle delay was 1 s. The NMR spectra were referenced to $[Al(H_2O)_6]^{3+}$.

Thermal analysis: Thermogravimetry, TG and Differential Scanning Calorimetry, DSC studies were performed on Thermobalance, TG50 and on differential scanning calorimeter, DSC 822 (Mettler, Toledo) in the range 25–250 °C under nitrogen flow at a heating rate of 2 °C min^{-1}.

Raman spectra were measured on an In Via Raman microscope (Renishaw, New Mills). An argon laser was used as an excitation source, with excitation wavelength of 514 nm.

Extra High Resolution Scanning Electron Microscope (XHR-SEM) imaging was performed at 5 kV using a FEI XHR SEM, MagellanTM 400L (Eindhoven, Holland). The specimen was prepared by deposition of a drop of the ethanol suspension of the sample onto 400 mesh copper grid.

High Resolution Transmission Electron Microscope (HR-TEM) imaging was conducted using a JEM-2100F (Japan). HR-TEM imaging was performed at 200 kV. A drop of the ethanol suspension of the sample was deposited onto 400 mesh copper grids covered with a lacey carbon net.

Dynamic light scattering (DLS) tests were performed on a Nano-ZS Zetasizer (Malvern, UK). The sample was prepared by dispersing the alumina perhydrate nanoparticles (0.02 wt%) in deionized water. The sample was sonicated for 30 minutes before the measurement.

XRD measurements were performed on a D8 Advance diffractometer (Bruker AXS, Karlsruhe, Germany) with a goniometer radius 217.5 mm, Göbel Mirror parallel-beam optics, 2° Sollers slits and 0.2 mm receiving slit. XRD patterns from 5° to 75° 2θ were recorded at room temperature using CuKα radiation (k=1.5418 Å) under the following measurement conditions: Tube voltage of 40 kV, tube current of 40 mA, step scan mode with a step size of 0.02° 2θ and counting time of 1 s/step. XRD patterns were processed using Diffrac Plus software.

Computational Section

All calculations reported in this work were carried out using Gaussian 09 program package.[61] Geometries were optimized at the MP2 level using aug-cc-pVDZ basis set for all of the atoms. Since alumina and silica are always aquated, optimizations were carried out in a simulated aqueous solvent by means of the polarizable continuum model (PCM).[62] Frequency calculations were carried out to verify that the final structures are indeed local minima. Single point energy calculations using the level and the basis set described above without solvent corrections were subsequently carried out. All results were corrected by the basis set superposition error (BSSE) which was calculated using the Boys-Bernardi counterpoise approach.[63] The electron density at the hydrogen bond critical point was calculated from the MP2 wavefunction using the PROAIM package.[64,65]

Alumina and silica were modeled as dimers. In the alumina case each aluminum atom was hexacoordinated. That is, the two aluminum atoms were bridged by two hydroxyl groups and each was further coordinated to two hydroxyl and two water groups, resulting in a neutral system. The decision to use hexacoordinated aluminum atoms was based on the ^{27}Al NMR of the alumina hydrogel presented in Figure 2. In the silica model on the other hand, each silicon atom was tetracoordinated. Here, an oxo bridge connects two silicon atoms, and each is further coordinated to three hydroxyl groups, again resulting in a neutral structure.

The structures of the alumina/silica dimers, as well as H_2O_2 and H_2O, were optimized separately and in complex. Due to the large number of degrees of freedom, different initial positioning of H_2O_2 or H_2O relative to the alumina/silica dimer served for the optimization of the complex, resulting in various possible model structures for the hydrate/perhydrate. Typical structures with the lowest energies are presented in this work. The stabilization and interaction energies (SE and IE, respectively) due to hydrate/perhydrate formation were calculated using Eq. 3:

$$\Delta E = E_{complex} - [E_1 + E_2] \qquad (3)$$

where $E_{complex}$ is the total energy of the hydrate/perhydrate, E_1 is the energy of H_2O/H_2O_2 and E_2 is the energy of the alumina/silica dimer. To calculate the SE, E_1 and E_2 involved the energies of the respective fragments in their fully optimized geometry. The IE on the other hand involved E_1 and E_2 of the fragments in their respective geometries within the complex.

Conclusions

We showed that an alumina hydrogel can function also as a

hydrogen peroxide carrier with high thermal and aqueous stability and also obtained alumina perhydrate nanoparticles with similar properties. This is the first stable perhydrate hydrogel and also the first stable aluminum peroxosolvate.

A comparison between the hydrogen bond features and the stabilization energies of the hydrate and perhydrate of silica and alumina clearly indicated a higher stability of alumina perhydrate in aqueous solution. On the matrix side, the higher coordination number of alumina provides a larger number of bonding sites, and the lower acidity of the aluminol groups makes them stronger HB acceptors compared to the silanol groups. Additionally, hydrogen peroxide forms stronger H–donor HBs than water and the rotation around the O-O axis of HOOH allows superior HB geometries compared to water. Finally, hydrogen peroxide can form more H- acceptor HBs.

The high stability of peralumina in aqueous solutions opens the door for water cleansing reactions and biocidal applications.

Acknowledgements

This research is supported by the Singapore National Research Foundation under CREATE programme Nanomaterials for Energy and Water Management, by the Israel Ministry of Science and the Energy Research Institute at Nanyang Technological University. We thank The Harvey M. Krueger Family Center for Nanoscience and Nanotechnology of the Hebrew University of Jerusalem and the Israel Science Foundation. We thank the Russian Foundation for Basic Research (grant 14-03-00279), the Council on Grants of the President of the Russian Federation (NSh-1670.2012.3), the Target Programs for Basic Research of the Presidium of the Russian Academy of Sciences and the Division of Chemistry and Materials Science of the Russian Academy of Sciences.

Notes and references

[a] *The Casali Institute of Applied Chemistry, The Institute of Chemistry, The Hebrew University of Jerusalem, Jerusalem 91904, Israel*
[b] *Institute for Drug Research, School of Pharmacy, Faculty of Medicine, The Lise-Meitner Minerva Center for Computational Quantum Chemistry, The Hebrew University of Jerusalem, Jerusalem 91120, Israel*
[c] *Kurnakov Institute of General and Inorganic Chemistry, Russian Academy of Sciences, Leninskii prosp.31, Moscow 119991, Russia.*
[d] *Department of Environmental Health Sciences, Hadassah Academic College, Jerusalem, Israel*
†Electronic Supplementary Information (ESI) available. See DOI: 10.1039/b000000x/

1. H. Nohl and W. Jordan, *Eur. J. Biochem*., 1980, **111**, 203.
2. S. Asada, K. Fukuda, M. Oh, C. Hamanishi and S. Tanaka, *Inflamm. res*., 1999, **48**, 399.
3. B. E. Watt, A. T. Proudfoot and J. A. Vale, *Toxicol. Rev*., 2004, **23**, 51.
4. C. W. Jones, *Applications of Hydrogen Peroxide and Derivatives*, ed. J. H. Clark, RSC, Cambridge, 1999. pp. 39.
5. W. C. Schumb, C. H. Satterfield and R. L. Wentworth, *Hydrogen peroxide*, Reinhold Publishing Corporation, New York, 1955.
6. M. L. Kuznetsov, Y. N. Kozlov, D. Mandelli, A. J. L. Pombeiro and G. B. Shul'pin, *Inorg. Chem.*, 2011, **50**, 3996.
7. J. Y. Piquemal, E. Briot and J. M. Brégeault, *Dalton Trans*., 2013, **42** , 29.
8. J. Weiss, *Adv. Catal.* 1952, **4**, 343.
9. J. Abbot and D. G. Brown, *Int. J. Chem. Kinet.* 1990, **22**, 963.
10. A. V. Churakov, S. Sladkevich , O. Lev, T. A. Tripol'skaya and P. V. Prikhodchenko, *Inorg. Chem*., 2010, **49**, 4762.
11. S. Sladkevich, J. Gun, P. V. Prikhodchenko, V. Gutkin, A. A. Mikhaylov, A. G. Medvedev, T. A. Tripol'skaya and O. Lev, *Carbon*, 2012, **50**, 5463.
12. A. MeKillop and W. R Sanderson, *Tetrahedron*. 1995, **51**, 6145.
13. S. Sladkevich, V. Gutkin, O. Lev, E. A. Legurova, D. F. Khabibulin, M. A. Fedotov, V. Uvarov, T. A. Tripol'skaya and P. V. Prikhodchenko, *J. Sol-Gel Sci. Technol*., 2009, **50**, 229.
14. Y. Wolanov, P. V. Prikhodchenko, A. G. Medvedev, R. Pedahzur and O. Lev, *Environ. Sci. Technol*., 2013, **47**, 8769.
15. P. V. Prikhodchenko, A. G. Medvedev, A. A Mikhaylov, T. A. Tripol'skaya, L. Cumbal, R. Shelkov, Y. Wolanov and J. Gun, *Mater. Lett*., 2014, **116**, 282.
16. J. Kaneko, S. Inoue, S. Kawakami and H. Sano, *J Endod*., 2000, **26**, 25.
17. A. McKillop and W. R. Sanderson, *Tetrahedron*, 1995, **51**, 6145.
18. C. J. Fritchie JR, and R. K. McMullan,. *Acta Crystallogr*., 1981, **B37**, 1086.
19. J. E. Dahl and U. Pallesen, *Crit. Rev. Oral. Biol. Med*., 2003, **14**, 292.
20. M. S. Cooper, H. Heaney, A. J. Newbold and W. R. Sanderson, *Synlett*, 1990, **9**, 533.
21. W. Adam and C. M. Mitchell, *Angew. Chem. Int. Ed.*, 1996, **35**, 533.
22. M. V. Vener, A. G. Medvedev, A. V. Churakov, P. V. Prikhodchenko, T. A. Tripol'skaya and O. Lev, *J. Phys. Chem. A*, 2011, **115**, 13657.
23. A. V. Churakov, P. V. Prikhodchenko, J. A. K. Howard and O. Lev, *Chem. Commun*., 2009, **28**, 4224.
24. P. V. Prikhodchenko, A. G. Medvedev, T. A. Tripol'skaya, A. V. Churakov, Y. Wolanov, J. A. K. Howard and O. Lev, *Cryst. Eng. Comm*., 2011, **13**, 2399.
25. Y. Wolanov, O. Lev, A. V. Churakov, A. G. Medvedev, V. M. Novotortsev and P. V. Prikhodchenko, *Tetrahedron*, 2010, **66**, 5130.
26. C. J. Brinker and G. W. Scherer, *Sol-Gel Science: The Physics and Chemistry of Sol-Gel Processing,* Academic Press, San Diego, 1990.
27. D. Avnir, T. Coradin, O. Lev and J. Livage, *J. Mater. Chem*., 2006, **16**, 1013.
28. J. Gun, O. Lev , O. Regev and A. Kucernak, *J. Sol–Gel Sci. Technol*., 1998, **13**, 189.
29. J. Zegli´nski, G. P. Piotrowski and R. Pieko´s, *J. Mol. Struct.*,2006, **794**, 83
30. J. Zeglin´ski, A. Cabaj, M. Strankowski, J. Czerniak and J. T. Haponiuk *Colloids Surf*., B, 2007, **54**, 165.
31. S. D. Kinrade, D. G. Holah , G. S. Hill , K. E. Menuz and C. R. Smith, *J. Wood. Chem. Technol*., 1995, **15**, 203
32. R. Rinaldi, F. Fujiwara, W. Holderich and S. Ulf, *J. Catal*., 2006, **244**, 92.
33. M. C. A. van Vliet, D. Mandelli, I. W. C. E. Arends, U. Schuchardt and R. A. Sheldon, *Green. Chem*., 2001, **3**, 243.
34. R. Rinaldi, H. F. N. de Oliveira, H. Schumann and U. Schuchardt, *J. Mol. Cata., A*, 2009, **307**, 1.
35. D. Mandelli, K. C. Chiacchio, Y. N. Kozlov and G. B. Shul'pin, *Tetrahedron Lett*., 2008, **49**, 6693.
36. J. E. Leffler and D. W. Miller, *J. Am. Chem. Soc*., 1977, **99**, 480.
37. H. M. Kao, R. R. Wu, T. Y. Chen, Y. H. Chen and C. S. Yeh, *J. Mater. Chem*., 2000, **10**, 2802.
38. J. J. Fitzgerald, in *Solid-State NMR Spectroscopy of Inorganic Materials*, ed. J. J. Fitzgerald ,ACS Symposium Series 717, American Chemical Society, Washington, DC, 1999, ch. 5, pp.182-196.
39. T. W. Swaddle, J. Rosenqvist, P. Yu, E. Bylaska, B. L. Phillips and W. H. Casey, *Science*, 2005, **308**, 1450.
40. L. F. Nazar and L. C. Klein, *J. Am. Ceram. Soc*., 1988, **71**, C-85.
41. W. S Szulbinski, *Spectrochim. Acta A*, 2000, **56**, 2117 – 2124.
42. K. Nakamoto, *Infrared and Raman Spectra of Inorganic and Coordination Compounds: Part B*, WILEY, New Jersey, 6nd edn., 2009.
43. C. J. Doss and R. Zallen, *Phys. Rev. B*, 1993, **48**, 15626.

44. Y. S. R. Chen, J. N Butler and W. Stumm W, *J. Colloid. Interface. Sci*. 1973, **43**, 421.
45. T. J. Van Emmerik, D.E Sandstrom, O.N. Antzutkin, , M. J. Angove and B. B Johnson, , *Langmuir*, 2007, **23**, 3205.
46. Y. Yang, Y.Q. Zhao and A.O. Babatunde. *Sep. Purif. Technol*., 2006, **51**, 193.
47. X. H. Guan, Q. Liu, G. H. Chen and C. Shang, *J. Colloid. Interface. Sci*., 2005, **289**, 319.
48. P. Borm, F. C. Klaessig, T. D. Landry, B. Moudgil, J. Pauluhn, K. Thomas, R. Trottier and S. Wood, *Toxicol. Sci*. 2006, **90**, 23.
49. T. Steiner, *Angew. Chem. Int. Ed*., 2002, **41**, 48.
50. S. J. Grabowski, *J. Mol. Struct*. 2001, **562**, 137.
51. O. MoÂ, M. YaÂnÏez and J. Elguero, *J. Chem. Phys*., 1992, **97**, 6628.
52. R. Parthasarathi, V. Subramanian and N. Sathyamurthy, *J. Phys. Chem. A*, 2006, **110**, 3349.
53. N. A. Chumaevskii, P. V. Prikhodchenko,N. A. Minaeva, and E. G. Ippolitov, *Rus. J. Inorg. Chem*., 2003, **48**, 1538.
54. J. Flanagan, W. P. Griffith, R. D. Powell, and A. P. West, *J. Chem. Soc. Dalton Trans*., 1989, **9**, 1651.
55. A.G. DiPasquale and J. M. Mayer, *J. Am. Chem. Soc*., 2008, **130**, 1812.
56. G. A. Kirakosyan, S. V. Loginov, T. V. Galuzina, V. P. Tarasov and Y. A. Buslaev, *Zhurnal Neorganicheskoi Khimii*, 1990, **35**, 2306.
57. R. Pizer and C. Tihal, *Inorg. Chem*., 1987, **26**, 3639.
58. I. I. Vol'nov, *Peroxides, Superoxides, and Ozonides of Alkali and Alkaline Earth Metals*, ed. A. W. Petrocelli, Plenum press, New York, 1966, pp. 79-86.
59. T. Ogihara, and H. Nakajima, *J. Am. Ceram. Soc*., 1991, **74**, 2263.
60. W. C. Schumb, C. H. Satterfield and R. L. Wentworth, *Hydrogen peroxide*, Reinhold Publishing Corporation, New York, 1955, pp. 553.
61. F. Gaussian 09 Revision A.1, M. J. Frisch, G. W. Trucks, H. B. Schlegel, G. E. Scuseria, M. A. Robb, J. R. Cheeseman,G. Scalmani,V. Barone,B. Mennucci, G. A. Petersson, H. Nakatsuji,M. Caricato, X. Li, H. P. Hratchian, A. F. Izmaylov,J. Bloino,G. Zheng, J. L Sonnenberg, M. Hada,M. Ehara, K. Toyota, R. Fukuda, J. Hasegawa, M. Ishida, T. Nakajima, Y. Honda, O. Kitao, H. Nakai, T. Vreven, Jr., J. A. Montgomery, J. E Peralta, F. Ogliaro, M. Bearpark, J. J. Heyd, E. Brothers, K. N. Kudin, V. N. Staroverov,R. Kobayashi,J. Normand, K. Raghavachari, A. Rendell, J. C. Burant, S. S Iyengar, J. Tomasi, M. Cossi, N. Rega, N. J. Millam, M. Klene, J. E. Knox, J. B. Cross, V. Bakken, C. Adamo, J. Jaramillo, R. Gomperts, R. E. Stratmann, O. Yazyev, A. J. Austin, R. Cammi, C. Pomelli, J. W. Ochterski, R. L. Martin, K. Morokuma, V. G. Zakrzewski, G. A. Voth, P. Salvador, J. J. Dannenberg, S. Dapprich, A. D. Daniels, Ö. Farkas, J. B. Foresman, J. V. Ortiz, J. Cioslowski and D. J. Fox, Gaussian, Inc., Wallingford CT, 2009.
62. S. Miertus, E. Scrocco and J. Tomasi, *J. Chem. Phys*., 1981, **55**, 117.
63. S. F. Boys and F. Bernardi, Mol. Phys., 1970, **19**, 553.
64. F. W. Biegler-König, R. F. W. Bader, and T.-H. Tang, *J. Computational Chem*., 1982, **13**, 317.
65. R. F. W. Bader, T.-H. Tang and F. W. Biegler-Konig, *J. Am. Chem . Soc*. 1982 , **104** ,946.